Advances in Engineering Software 99 (2016) 81–88

Contents lists available at ScienceDirect

Advances in Engineering Software

journal homepage: www.elsevier.com/locate/advengsoft

Research paper

Finite element mapping for incompatible FE meshes of composite structures

Natalie Mayer[a,*], Björn Van Den Broucke[b], Jens Prowe[b], Tamas Havar[b], Roland Hinterhölzl[a]

[a] Institute for Carbon Composites, Faculty of Mechanical Engineering, Technische Universität München, Boltzmannstr. 15, D-85748 Garching b. München, Germany

[b] Department of Structure Engineering, Production and Aeromechanics, AIRBUS Group Innovations, Willy-Messerschmitt-Straße 1, D-81663 Ottobrunn, Germany

ARTICLE INFO

Article history:
Received 13 December 2015
Revised 27 April 2016
Accepted 13 May 2016
Available online 25 May 2016

Keywords:
Mapping
Finite element analysis
Finite element data transfer
Composite structures
Manufacturing chain simulation
Integrated simulation approach
Structural analysis

ABSTRACT

Finite element analysis (FEA) of structural composites is mostly based on an as-designed geometry and input data. As-designed input data do not consider the manufacturing processes. For an as-built structural simulation of composites, it is important to integrate manufacturing process data into the structural analysis. Therefore, mapping algorithms are needed to transfer and process data between different process and structural simulation steps considering the application of different finite elements and media discretization for the individual simulation steps. This paper considers a mapping algorithm based on a bucket sort algorithm, shape interpolation functions of finite elements and internal fiber architectures of composite materials with a subsequent material properties prediction. The proposed algorithm is applicable for unidirectional composites as well as for non-crimped, woven and braided fabrics. Particular, it is shown how fiber orientation, as vector value of finite elements, is sensible for a data transfer between meshes with out-of-plane material defects. This integrated simulation approach is applied on a generic demonstrator geometry and aerospace component geometries. The implementation is realized within a new developed simulation platform for composites structures, from process up to structural simulations.

1. Introduction

Finite element analysis (FEA) is a common instrument to design and analysis composite structures. Several engineering simulation packages are available in specific engineering fields for mechanical, thermo-mechanical or fluid dynamics analyses. A multidisciplinary FEA of composite structures is important for a realistic simulation of structural behavior. The multidisciplinary FEA consider a combination of different approaches for process and structural simulation and can use shell, plate, beam or solid element theories. The mesh and element diversity makes it difficult to combine different approaches and to analyse effects of manufacturing effects and defects [1–3]. Several strategies were developed to transfer FE data between shell element meshes [4,5] or between shell and solid element meshes [6]. Approaches for a data transfer between different simulations for fluid dynamics and structural simulations of metal components have been presented [7,8,9,10]. In the analysis of composite structures, process simulations are less integrated into structural simulations.

The manufacturing chain of composites includes i.e. preforming, impregnation and curing processes. The manufacturing processes are simulated with several finite element (FE) packages based on shell and solid element meshes, where FE and meshing strategies are depending on the engineering problems. A preforming step can be done with a draping, a braiding or an automated fiber placement (AFP) process. Composite materials do not fit exactly a desired geometry during a draping process and can produce wrinkling material defects [11]. FE based draping simulations can reproduce out-of-plane wrinkling and shear behavior of composite materials. Such simulations use separated meshes per composite ply [12] with material parameters and contact definitions. Results of these simulations are represented on a deformed mesh geometry compared to the designed geometry. Therefore, the draping mesh is incompatible with a structural mesh where a shell element mesh based on the designed geometry is used for all layers. If the source and the target meshes have different FE geometries then the produced mapping errors are more relevant for the next analysis steps. The main challenge here is to map the fiber orientations of the source mesh as vectors into a new reference coordinate system and reproduce manufacturing effects and defects of materials. The different source reference coordinate systems are used in applications such as structural simulations

* Corresponding author.
E-mail address: mayer@lcc.mw.tum.de (N. Mayer).

http://dx.doi.org/10.1016/j.advengsoft.2016.05.007
0965-9978/

based on process data or process simulations based on measuring data [13].

Commercial software packages [14–18] implemented different solutions in this field. A main limitation of these solutions is that these packages transfer fiber orientation values from kinematic draping simulations. Kinematic draping approaches are geometry or energy based and the results are represented on the same FE geometry as a structural FE geometry. A kinematic draping approach is used for a first estimation of a draping behavior. On the other hand, FE- or mechanically based draping simulations are used for more realistic behavior estimations. The existing commercial mapping solutions cannot be extended with other software packages. However, it is important to use a software-independent mapping solution for a multidisciplinary analysis of composite structures to understand a composite material behavior with different simulation approaches.

The need of a manufacturing simulation chain for composite components is growing in the last years in the industry because of manufacturing costs and process time optimization. Recent publications show the interest on a simulation chain for composites components in the automotive industry. Different established methods were combined for a multi-level analysis of process manufacturing chains up to structural simulation for unidirectional fiber reinforced composite components [19–23]. The aim of the present paper is to show how it is possible to map FE draping simulation results of the composite structures into structural analysis with different software packages and for different material textile structures. Especially, it is shown how to use the shape functions for element-to-node transfer and how to calculate additional properties with no auxiliary meshes, how to transfer scalar, vector and tensor values and how to predict material properties of the composite materials based on the mapping results. The procedure follows an approach based on the methods published in [24–28] using a global searching algorithm based on bucket sort techniques and a point-element testing with FE shape functions. Subsequent projection and interpolation methods are applied for a transfer of nodal or element values to integration or centroid points of elements. Material properties prediction is used for the calculation of stiffness values for sheared woven fabrics with an approach extended from a well-known model of Ishikawa et al. [29,30]. This approach allows including shear draping information into material properties on a meso-macro scale and provides a more efficient calculation compared to the FE unit cell methods. Based on the first investigation results published in [31–33], the mapping process was developed and applied to unidirectional and woven industrial composite components [34–36].

In this paper, the following Section 2 describes mapping methods and properties calculation based on mapping results. Aerospace and academic applications are discussed in Section 3. A section describing the obtained results is followed by conclusions.

2. Methods

This chapter discusses the main steps of the developed mapping algorithm for composite components. This mapping algorithm was applied on a predefined exchange format for FE data for composite structures inside a simulation platform. The concept of the simulation platform with a virtual process chain from draping up to structural analysis with some examples of software tools is shown in Fig. 1. This concept is not only limited to commercial software but can also be used with open source solutions. In the first step, FE simulation results based on as-designed parameters are transferred into the common commercial software neutral exchange data format with forward wrapping tools. In the second step, the mapping algorithms are applied on these results for a data transfer between different simulations. Finally, the mapping results are

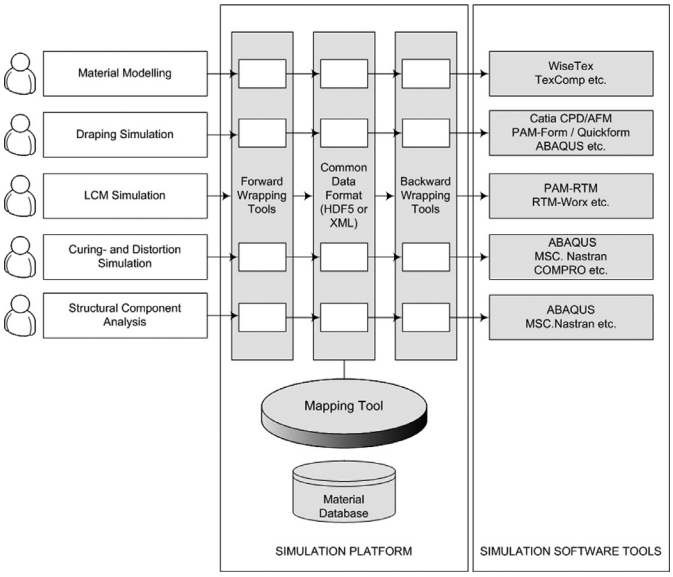

Fig. 1. Simulation platform for composites.

transferred into a simulation data format with backward wrapping tools for as-built simulations. As-built FEA is using shell, solid elements etc. with the defined fiber orientations and the assigned material properties.

For example, Fig. 2 presents two incompatible meshes from draping and structural simulations on a generic part with two plies. Instead of a structural mesh, e.g. shell or solid element meshes for the impregnation and curing simulations can be used. FE draping plies are represented separately. The structural simulation is employing a mesh based on the designed geometry using composite layered shell elements. The aim is to transfer FE fields (fiber orientation, thickness, shear angle, etc.) as output from FE-based draping simulation assigned to every element or node (source mesh) into a new structural mesh (target) and define the new material input data for an as-built analysis.

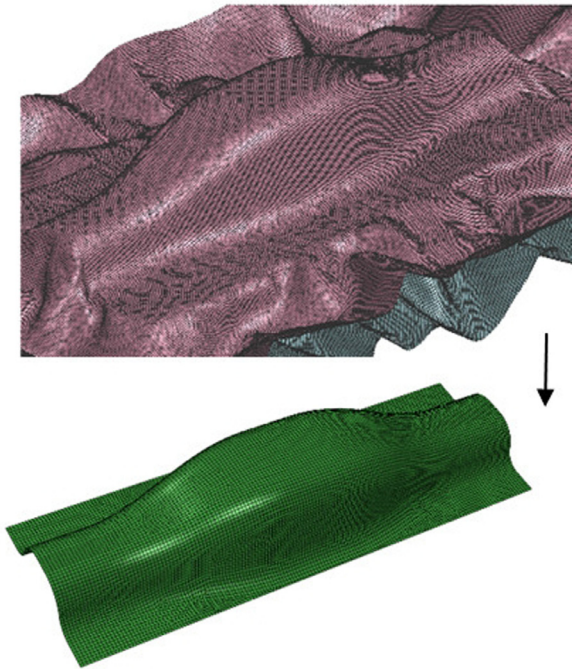

Fig. 2. Draping (top) and structural (bottom) meshes.

Fig. 3 shows the road map of the applied methods in this paper for the mapping algorithm with different incompatible FE meshes. First, source and target meshes are compared geometrically. A search algorithm is applied to find the reference source elements with as-built data. Second, FE source data are transferred onto a target mesh. Third, due to an out-of-plane mesh incompatibility, source fiber orientations are projected onto the target mesh elements. Finally, methods for a stiffness prediction for woven fabrics are applied. Every step of this road map is discussed in the following subsections.

2.1. Searching methods

For a data transfer from a source mesh onto a target mesh a representative point-element pair (target-source pair) is defined for every composite ply of the composite component. Different techniques can be applied for a transfer of calculation results between source and target nodes, integration points or centroid points of elements. For example, the nearest point method [37,38] is used for a quick and efficient transfer for meshes with small geometric deviations. However, an approach is needed for a data transfer between incompatible meshes for draping and structural simulations, which can reduce the number of transfer errors of FE data. Therefore, a technique based on the FE shape functions is applied. The following methods can find a corresponding element of a source mesh for a point of a target mesh where meshes represent different geometries and use different elements:

- Global bucket sort algorithm [24–26]
- Extended theory search [28]
- Local point-element testing [39]

At first, a global three-dimensional bucket sort algorithm with a local extended territory search is applied. To speed up a searching procedure, the meshes are divided in the buckets by coordinates of the source and target nodes. These buckets include the references to FE nodes (Fig. 4). The number of a bucket for a source or a target node with the coordinates (x, y, z) is defined as follows:

$$N_{B_x} = \left\lfloor \frac{x_{max} - x_{min}}{W} \right\rfloor + 1, \tag{2.1}$$

$$N_{B_y} = \left\lfloor \frac{y_{max} - y_{min}}{W} \right\rfloor + 1, \tag{2.2}$$

$$N_{B_z} = \left\lfloor \frac{z_{max} - z_{min}}{W} \right\rfloor + 1, \tag{2.3}$$

where x_{max}, x_{min}, y_{max}, y_{min}, z_{max}, z_{min} are maximal and minimal coordinates of source or target nodes and W is a characteristic length

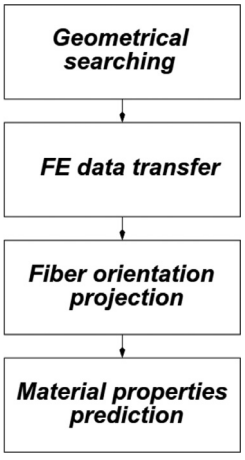

Fig. 3. Road map of the applied methods.

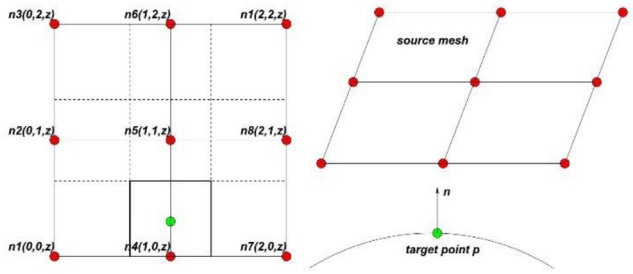

Fig. 4. Source mesh with buckets (bold) (left). Average normal of the target node (right).

of the element edge, here W= 0.7. A bucket number for a source or a target node i with coordinates (x_i, y_i, z_i) is defined as follows:

$$B_x^i = \left\lfloor \frac{x_i - x_{min}}{W} \right\rfloor + 1, \tag{2.4}$$

$$B_y^i = \left\lfloor \frac{y_i - y_{min}}{W} \right\rfloor + 1, \tag{2.5}$$

$$B_z^i = \left\lfloor \frac{z_i - z_{min}}{W} \right\rfloor + 1. \tag{2.6}$$

A list of source elements inside of every bucket is created if at least one node of these elements lies inside a bucket. Every element may be inside multiple buckets or may have multiple nodes in the same bucket. However, the node should be listed once to perform the next operations, efficiently.

In the second step, the distance between all points of the target mesh (nodes or integration points) is compared to the source elements. The average normals of the nodes are used for a point-element testing. The searching for a corresponding element in the extending territory of the element is realized according to the Zhong and Nilsson theory [28]. An element is considered as a candidate for a point-element pair if the target point is located inside the extended territory of this source element:

$$x_{min}^e \le p_x \le x_{max}^e, \tag{2.7}$$

$$y_{min}^e \le p_y \le y_{max}^e, \tag{2.8}$$

$$z_{min}^e \le p_z \le z_{max}^e, \tag{2.9}$$

with

$$x_{min}^e = \min_{i=1,N_e} x_i - \varepsilon,\ x_{max}^e = \max_{i=1,N_e} x_i + \varepsilon, \tag{2.10}$$

$$y_{min}^e = \min_{i=1,N_e} y_i - \varepsilon,\ y_{max}^e = \max_{i=1,N_e} y_i + \varepsilon, \tag{2.11}$$

$$z_{min}^e = \min_{i=1,N_e} z_i - \varepsilon,\ z_{max}^e = \max_{i=1,N_e} z_i + \varepsilon, \tag{2.12}$$

where (p_x, p_y, p_z) are coordinates of the target point.

In cases where the point p is located at a certain distance from the element, the point-element pair will be neglected for a further processing. If the point should be considered, the extended territory has to be calculated based on the maximum coordinates of the element that is growing in a thickness direction by a certain searching radius.

The local point element testing based on the FE shape functions identifies the local coordinates (ξ, η, μ) of the target point p regarding the source element of each point-element pair candidate. The position of this point p can be expressed as

$$\boldsymbol{p} = \boldsymbol{x}^s(\xi, \eta) + \mu \boldsymbol{n}^s(\xi, \eta), \tag{2.13}$$

where:

$$\boldsymbol{x}^s(\xi, \eta) = \sum_{i=1}^{N} N_i^s(\xi, \eta) \boldsymbol{x}_i^s \tag{2.14}$$

and the element normal $n^s(\xi,\ \eta)$:

$$\boldsymbol{n}^s(\xi,\eta) = \sum_{i=1}^{N} N_i{}^s(\xi,\eta)\boldsymbol{n}_i^s \tag{2.15}$$

with the interpolation functions of the FE: $N_i{}^s(\xi,\ \eta)$, the source node coordinates: $\boldsymbol{x}_i^s$ and the average normal of the node i: $\boldsymbol{n}_i^s$.

The local coordinates $(\xi,\ \eta,\ \mu)$ of the point p are determined iteratively by minimizing the distance between the real coordinate of p and the coordinate determined by Eq. (2.13) [39]. A tested source element in a candidate point-element pair is considered a matching element if the found local coordinates $(\xi,\ \eta)$ are in the range from -1 to $+1$. The third local coordinate μ can be used to calculate the distance between the point p and the source element according to

$$\mathrm{d} = \|\mathbf{p} - \boldsymbol{x}^s\| = \|\mu \boldsymbol{n}^s(\xi,\eta)\| \tag{2.16}$$

2.2. Data transfer

Transfer of the calculation results between the source and target nodes, integration or centroid points of elements is using the FE interpolation functions. Every point p is using the source element values based on the local coordinates. In case of a nodal value transfer, the new value at the point p is defined as follows:

$$f_j^d = \sum_{i=1}^{N_e} N_i{}^s(\xi,\eta) f_i^s, \tag{2.17}$$

where f_i^s is the source value at the node, N_e a number of the source element nodes and f_j^d the new value of the target node. Here, $(\xi,\ \eta)$ are the indicated local coordinates of the target node j with respect to the corresponding source element.

Data transfer from the integration points is realized with extrapolation functions. The field value in an integration point f_g^d can be calculated as follows:

$$f_g^d = \sum_{i=1}^{N_e} N_i{}'^s(\xi,\eta) f_i^s, \tag{2.18}$$

where $N_i{}'^s(\xi,\eta)$ is the extrapolation function.

The FE interpolation or extrapolation functions with the weighted or unweighted averaging techniques are used for a relocation of data between nodes and integration points. The weighted averaging depends on the type and the geometry of the element.

2.3. Projection method for fiber orientation fields

The fiber orientation field is a vector value in a global or defined local coordinate system. Before the source field value is assigned to a target mesh, the fiber orientations have to be transformed into a global coordinate system. After this, the global fiber orientations are projected onto the new target element. It is important to take into account that the source elements and the target elements can be in different planes because of the mesh incompatibility (Fig. 5). A new target element value can be calculated with a pair-testing for a centroid or every node of this element with a subsequent averaging technique.

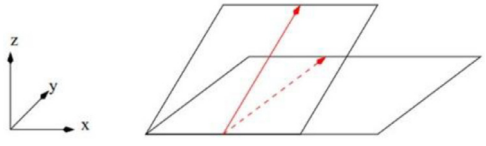

Fig. 5. Source element with the fiber orientation and target element are in different planes.

Fig. 6 shows possible draping simulation results with material defects such as fiber waviness or wrinkles. The manufacturing process can cause such defects. The FE based calculation, presented here, uses fabric material properties and friction properties between tooling and fabric layers, and is capable to reproduce shear angles and wrinkling defects of textile composite preforms [40]. These results have to be transferred onto a shell element structural mesh with a representation of these composite material defects.

The question is how big the influence of these defects on the material properties and the structural behavior [41]. A way studied in this paper is to determine in-plane effects on a structural mesh from out-of-plane wrinkling draping defects. A standard cross product projection is applied for the fiber orientation transfer. An another approximated solution could be a special projection method with parameters dependent on the angle between the source and target planes. However further research is needed on this topic. The achieved results are discussed in Section 4.

2.4. Material properties prediction for sheared woven structures

Composite materials distinguish between unidirectional (UD), non-crimped (NCF), woven and braided preforms. Two-dimensional NCF, woven or braided fabrics are widely used for automotive and aerospace applications. The architecture of these materials is established through on or several main yarns with crimp and undulation effects [42]. Therefore, the material properties prediction for such materials is defined on the material characterization results and the mechanics of composite materials that consider the geometry of the yarns. Fiber volume content (FVC) and mechanical properties as well as the stiffness and strength change with a high undulation factor and shear angle between yarns.

For an equivalent representation of material properties for the sheared fabrics in a structural analysis, e.g. an angle-ply approach with a knock down factor can be used [43]. To avoid the determination of the knock down factors experimentally, additional a smeared approach can be applied for the prediction of the material properties [42]. Several modeling technics for such an approach have been presented in the last years [29–44]. The information of a shear angle is mostly not used in the analytical approaches. On the other hand, different FE calculation approaches are existing for woven and braided fabrics [45,46]. These approaches can be applied also for sheared woven fabrics. However, it is usually too time consuming for industrial solutions. Therefore, well-known analytical approaches [29,30] are extended and compared for a sheared woven fabric stiffness prediction based on the mapping results. The

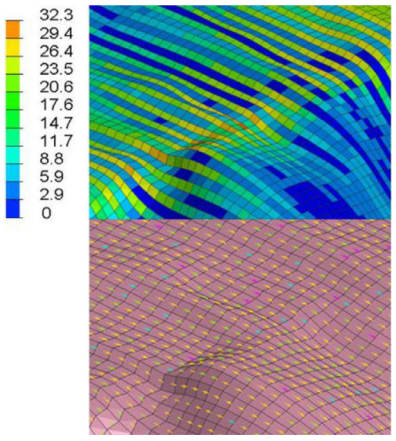

Fig. 6. FE-based draping results for a woven fabric. Shear angle distribution (top). Out-of-plane wrinkling with the weft fiber orientations (bottom).

validation of these approaches are done on woven fabric with RTM6 resin system with tensional tests for the shear angle set-ups of 5/10/15 and 25 degrees. These validation results have been presented in [36]. The method uses the model of Ishikawa et al. with reduced UD properties for a stiffness prediction corresponds with the validation results with minimal deviations. A unit cell representation of a woven fabric in this model contains a sinusoidal area for an undulation description and a straight area for a non-crimped yarn part. This approach can also be applied for a stiffness prediction of braided fabrics.

3. Mapping applications

Static or dynamic analysis and design of automotive or aerospace components is realized with FEA. The developed and implemented simulation platform for composite structures is used for a static structural analysis in the SIMULIA ABAQUS software package. FE-based draping simulations are performed with the ESI Group PAM-Form software package. To analyze how the draping results affect the structural behavior of a component on a macro level, several components with geometries ranging from simple up to complex are investigated.

3.1. A simple geometry

At first, simple source and target meshes are considered for a node information transfer. Here, the source and the target meshes are lying on the same surface and the meshe domains are discretisized into different elements. Fig. 7 shows the source and the target meshes. The source mesh contains the predefined scalar temperature information at the mesh nodes. The mapping results are presented in Section 4.

3.2. Industrial application

The following industrial applications are investigated together with industrial partners: a L-profile, a helicopter crash element (Fig. 8) and a helicopter frame (Fig. 9). The geometry of the L-profile is single curved. Therefore, in reality, the draping results for the L-profile show minimal fiber angle deviations up to four degrees from the nominal design. The crash element and the helicopter frame are more complex. Figs. 8 and 9 show the draping results for a +45°/–45° ply and structural meshes of these components. Both components are manufactured with several plies of woven fabrics. Here, the source and the target meshes feature an out-of-plane mesh incompatibly.

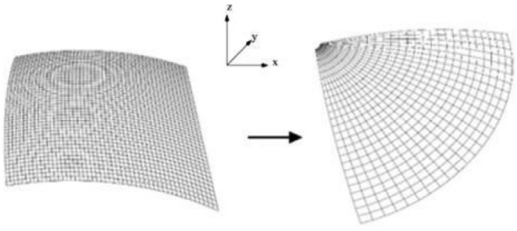

Fig. 7. Source mesh (left). Target mesh (right).

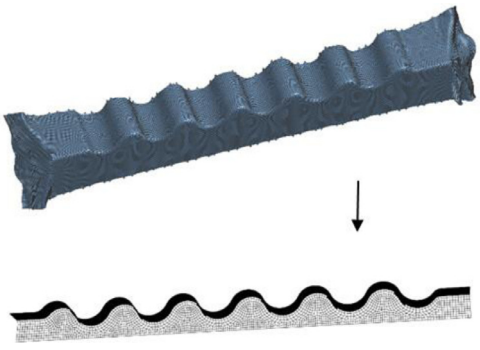

Fig. 8. Crash element: one draped source ply (top) and the target mesh (bottom).

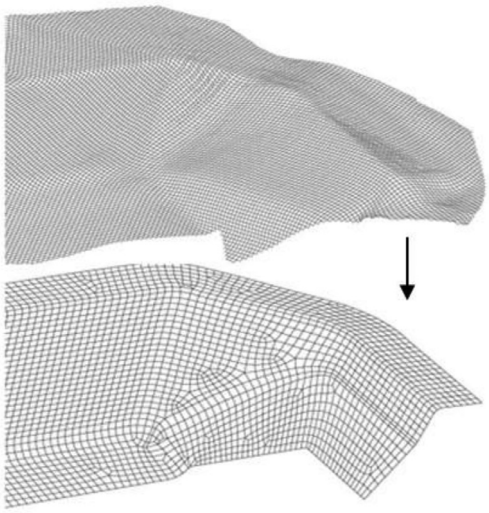

Fig. 9. Helicopter frame corner part: one draped source ply (top) and the target mesh (bottom).

3.3. A generic demonstrator

To analyse the mapping results on a complex double curved geometry, a representative generic geometry was designed. A complex generic geometry is considered for an investigation of a structural behavior with different lay-ups and process parameters. Here, one fabric ply is used for the lay-up. Fig. 10 shows the demonstrator geometry with the draping results from PAM-Form solver for a 0°/90° woven fabric ply and the target mesh for a structural analysis. A draping simulation is performed with a stamping approach. The mapping and static three point bending test results for this component are presented in Section 4.

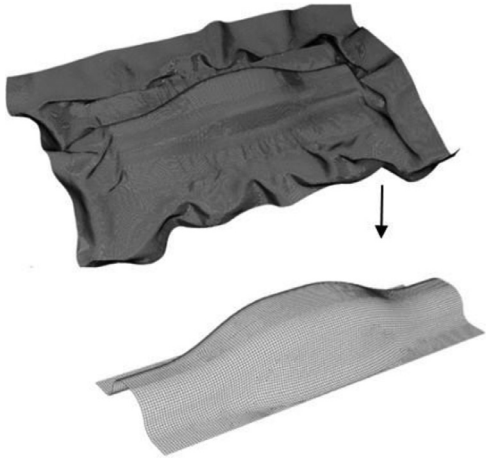

Fig. 10. A generic demonstrator: the draping results (top) and the structural mesh (bottom).

It should be noted, that in process simulations finer meshes in comparison to structural meshes or meshes with the same discretization as the structural mesh are recommended to minimize data transfer errors. In the case of a more coarsely source mesh wrong source element data can be chosen by the mapping in curved areas. Different element planes can influence the projection results of fiber orientations onto the target elements. If the mapping algorithm is applied to the target nodes instead of the element centroids, it is recommended to use similar discretizations for the source and target meshes.

4. Results

In this Section, the mapping results of the proposed mapping algorithms for node and element value transfer without and with mesh defects and a subsequent material properties prediction are presented.

4.1. Node value transfer

The node information can content scalar, vector or tensor values. Cure temperature, displacements and stresses are defined at every mesh point. Fig. 11 shows an example of temperature values defined on the source nodes and the transfer of these values onto a target mesh. This result shows the interpolation method based on the FE shape functions, which allows a minimal loss of transferred data.

4.2. Element values transfer

Here, we consider fiber orientation values that are defined during an FE-based draping simulation on the demonstrator geometry. The PAM-Form solver was used for a draping stamping process with a 0°/90° woven fabric ply. The fiber orientations for weft and warp fibers are given in a global coordinate system. A corresponding structural mesh is defined on the designed geometry with layered shell elements. The material orientations are defined locally on the element edges. Figs. 12 and 13 demonstrate the shear angle

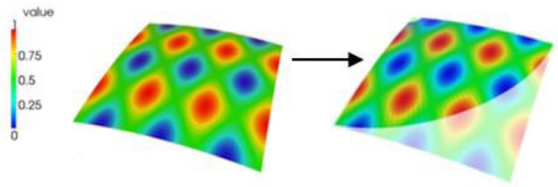

Fig. 11. The source (left) and target (right) meshes with temperature values at nodes.

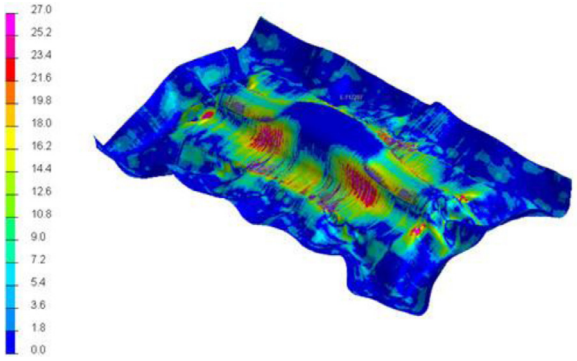

Fig. 12. Source mesh of the demonstrator: shear angle distribution.

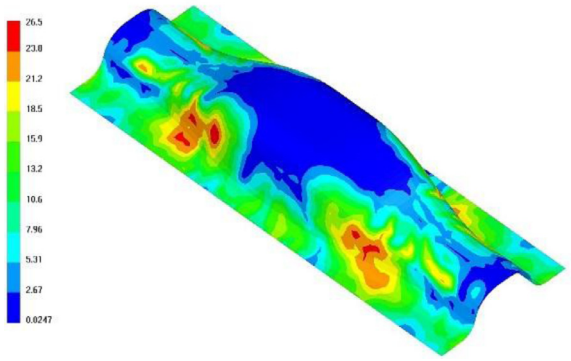

Fig. 13. Target meshes of the demonstrator: shear angle distribution [36].

distribution on the draping mesh and the mapped shear angle distribution on the structural mesh. The maximal shear angle of 26.5° is observed.

4.3. Effects of mesh defects

As discussed in Section 2, fiber orientations can be sensible for a transfer if the source or the target meshes content out-of-plain areas in relation to the initial geometry. In this example, a fragment of a source mesh with wrinkling defects of a woven fabric is shown. Fig. 14 illustrates such a fragment with the corresponding target mesh and demonstrates mapping results for warp and weft fiber orientations. The standard cross product projection is used for a projection of the source fiber orientations onto the target mesh. The mapped local fiber orientations are different to source orientations due to different finite elements in the source and target meshes. Furthermore, the out-of-plane defects influence the local orientations and therefore produce different orientations

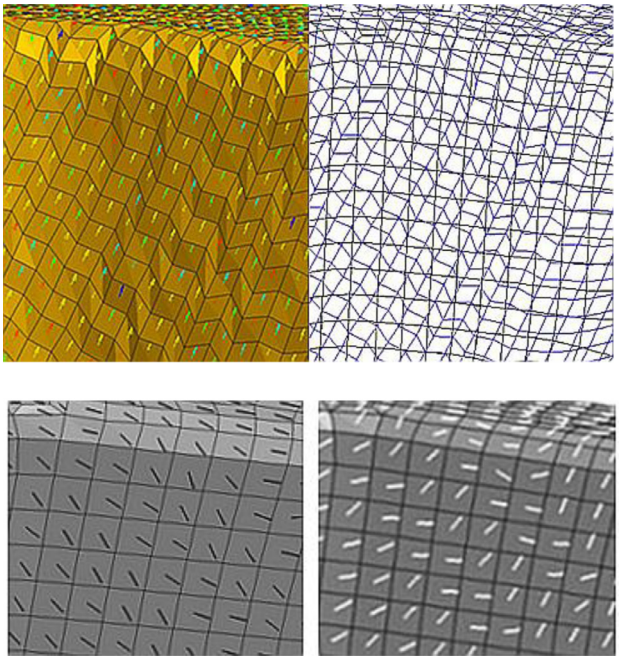

Fig. 14. Source draping mesh with the weft fiber orientation (top left). Source (black) and target (blue) meshes (top right). Target mesh with mapping results for the warp (bottom left) and weft (bottom right) fiber orientations.(For interpretation of the references to color in this figure legend, the reader is referred to the web version of this article.)

in neighboring elements. In general, out-of-plane wrinkling leads to in-plane-wrinkling on the structural mesh after the consolidation process. Here, the transfer of the fiber orientations increases the shear angle and stiffness values for some structural elements. FVC based on the fiber orientations and the thickness values is changing as well. In reality, a stiffness degradation is expected in these areas. Therefore, the wrinkling effect can be mapped only partially due to restrictions by the standard cross product projection method.

4.4. Stiffness prediction

To show how important it is to predict stiffness values for woven fabrics based on the mapping results, a three point bending test for the demonstrator is undertaken. The material prediction methods are applied for the target mesh. The stiffness prediction method from Section 2 defines the engineering constants in the material cards of the elements. A static structural analysis is performed for a three-point bending test on one 0°/90° woven epoxy ply with as-designed and as-built configurations. The load definition is a displacement of –1 mm applied at the top area of the geometry (Fig. 15).

Fig. 16 illustrates two load-displacement responses for simulation results based on following configurations: initial material properties for the woven fabric and material properties with the approach from Section 2 using mapping results for warp, weft fibers and thickness fields. These results show a difference of up to 38%.

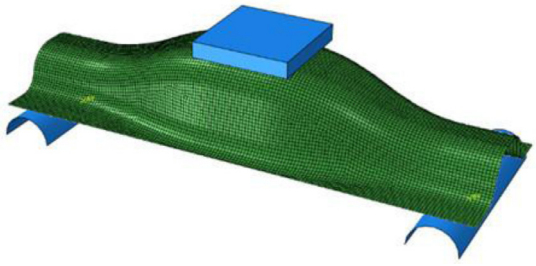

Fig. 15. Simulation of the three point bending test.

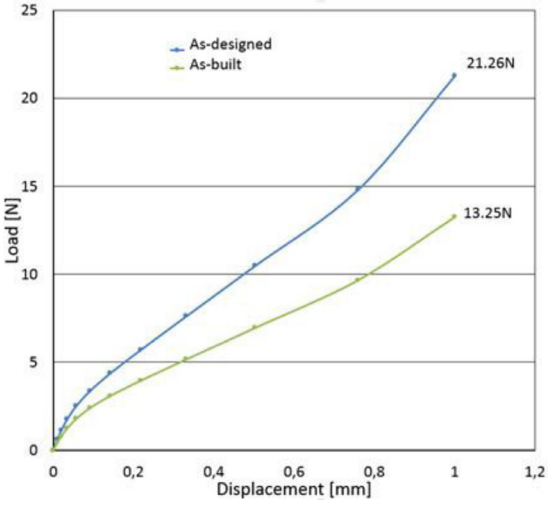

Fig. 16. The resulting load-displacement response for the as-designed and as-built configurations.

5. Conclusion

Process simulations of composite structures are seaming less integrated into structural analysis. This paper presented mapping algorithms with the focus on fiber orientation transfer for UD, NCF, woven or braided fabrics and subsequent material properties prediction between incompatible meshes. A definition of the fiber orientation needs a reference system that can be changed from mesh to mesh. Incompatible meshes from draping and structural analysis are discussed. Only the transfer of FE data is not sufficient for a realistic structural analysis and the subsequent design of complex components with e.g. draped UD, NCF, woven and braided fabrics. Stiffness predictions based on shear angle and thickness variation is shown with an extended validated analytical approach for the sheared woven composite materials.

The discussed methods are applied for a data transfer between draping, infiltration, curing and structural meshes. The solid element meshes are simplified to a shell surface representation. The implemented simulation platform for composite structures allows exchanging FE simulation data based on the predefined common data format and calculating additional properties: FVC, permeability and engineering constants. The common data format represents FE data from several FE solvers in a container data structure.

The material defects such as gaps, overlaps and out-of-plane wrinkling change stiffness and strength properties of the composite structure. The problem of the out-of-plane-winkling representation on a structural mesh is addressed for further detailed research due to restrictions by the standard projection method. The presented method is capable to determine weak areas partially of the composite part. The detected areas can be taken into account by a design step. If the target mesh is an deformed source mesh, then the mapping algorithm has to use a parametric projection for a data transfer. Furthermore, the proposed methods can be applied for the data exchange between manufacturing robots or measuring sensor data and simulation software packages for a detailed quality control of manufacturing processes.

Acknowledgments

This work was supported by the Federal Ministry of Economics and Technology under the Framework of the Aeronautics Research Program IV in the project CompTAB and by the MAI Carbon Cluster Excellence Initiative in the project MAI Design. Special acknowledgements are given to our project partners from AIRBUS Helicopters Deutschland, Dr. J.-M. Balvers and Mr. C. D-Angelo, and our students, Ms. A. Sodji, Mr. S. Heckelsmüller and Mr. M. Schroll.

We appreciate fruitful discussions and exchange on this topic with Prof. Dr. A.C. Long, Dr. A. Endruweit, Prof. Dr. A.A. Becker, Dr. M. Afazov and Dr. D. Scrimieri from the University of Nottingham, United Kingdom.

Furthermore, we would like to thank our team colleagues for the support.

References

[1] Tersing H, Lorentzon J, Francois A, Lundbäck A, Babu B, Barboza J, et al. Simulation of manufacturing chain of a titanium aerospace component with experimental validation. Finite Elem Anal Des 2012;51:10–21.
[2] Afazov S, Nikov S, Becker A, Hyde T. Manufacturing chain simulation of an aero-engine disc and sensitivity analyses of micro-scale residual stresses. Int J Adv Manuf Technol 2011;52:279–90.
[3] Ji J, Kim K, Seo M, Kim T, Park D, Kim Y, Ko K. Load mapping for seamless interface between hydrodynamics and structural analyses. Adv Eng Softw 2014;71:9–18.
[4] Fernandes J, Martins P. All-hexahedral remeshing for the finite element analysis of metal forming processes. Finite Elem Anal Des 2007;43:666–79.
[5] Bucher A, Meyer A, Goerke U-J, Kreissig R. A comparison of mapping algorithms for hierarchical adaptive FEM in finite elasto-plasticity.. Comput Mech 2007;39(4):521–36.

[6] Dureisseix D, Bavestrello H. Information transfer between incompatible finite element meshes: Application to coupled thermo-viscoelasticity. Comput Methods Appl Mech Eng 2006;195:6523–41.
[7] Scrimieri D, Afazov S, Becker A, Ratchev S. Fast mapping of finite element field variables between meshes with different densities and element types. Adv Eng Softw 2014;67(1):90–8.
[8] Ahrem R. Multidisciplinary simulations with the coupling library MpCCI. Online J PAMM 2002;1(1):39–42.
[9] Afazov S, Becker A, Hyde T. Development of a finite element data exchange system for chain simulation of manufacturing processes. Adv Eng Softw 2012;47(1):104–13.
[10] Afazov S. Modelling and simulation of manufacturing process chains. CIRP J Manuf Sci Technol 2013;6(1):70–7.
[11] Dangora LM, Mitchell CJ, Sherwood JA. Predictive model for the detection of out-of-plane defects formed during textile-composite manufacture. Compos Part A 2015;78:102–12.
[12] Boisse P, Hamila N, Vidal-Sallé E, Dumont F. Simulation of wrinkling during textile composite reinforcement forming. Influence of tensile, in-plane shear and bending stiffnesses.. Compos Sci Technol 2011;71:683–92.
[13] Heieck F, Fuhr J, Middendorf P. Quality assessment of 2D braided composites with optical measurement techniques. In: Proceedings of ICCS18, Lisbon; 2015.
[14] ANSYS. ACP Documentation, 15.5 edition, 2015.
[15] Dassault Systémes SE. Composite Modeler for ABAQUS Documentation, 6.14 edition, 2015.
[16] ESI Group. Visual Environment Documentation, 16.5 edition, 2015.
[17] BETA CAE Systems USA , Inc. ANSA, ANSA Documentation. 15.3.6 edition, 2015.
[18] MSC DIGIMAT . DIGIMAT-MAP Documentation, 6.0.1 edition, 2015.
[19] Dix M, Bickerton S, Tryfonifis M, Hinterhölzl R. Consistent virtual CFRP process chain using a modular CAE interface. In: Proceedings of NAFEMS world congress, Salzburg; 2013.
[20] Bulla A, Ehrhart F. A holistic simulation driven composite design process. In: Proceedings of NAFEMS seminar simulation of composites – a closed process chain, Leipzig; 2014.
[21] Kärger L, Fritz F, Magagnato D, Galkin S, Schön A, Oeckerath A, Wolf K, Henning F. Development stage and application of a virtual process chain for RTM components. In: Proceedings of NAFEMS seminar simulation of composites – a closed process chain, Leipzig; 2014.
[22] Fuhr J, Feindler N, Middendorf P. Virtual analysis of draping effects on stiffness and strength of ply-based composite structures. In: Proceedings of NAFEMS seminar simulation of composites – a closed process chain, Leipzig; 2014.
[23] Kärger L, Bernath A, Fritz F, Galkin F, Magagnato D, Oeckerath A, Schön A, Henning F. Development and validation of a CAE chain for unidirectional fibre reinforced composite components. Compos Struct 2015;132:350–8.
[24] Belytschko T, Kennedy J, Lin J. Three-dimensional penetration computation. Struct Mech React Technol 1987;1:83–7.
[25] Belytschko T, Lin J. A three-dimensional impact-penetration algorithm with erosion. Comput Struct 1987;25(1):95–104.
[26] Benson D, Hallquist J. A single surface contact algorithm for the post-buckling analysis of shell structures. Comput Methods Appl Mech Eng 1990;78(2):141–63.
[27] Belytschko T, Neal O. Contact-Impact by the pinball algorithm with penalty and lagrangian methods. Int J Numer Methods Eng 1991;31(3):547–72.
[28] Zhong Z-H, Nilsson L. Contact-impact algorithms on parallel computers. Nucl Eng Des 1994;150(2-3):253–63.
[29] Ishikawa T, Chou T-W. Stiffness and strength behaviour of woven fabric composites. J Mater Sci 1982;17:3211–20.
[30] Ishikawa T, Chou T-W. One-dimensional micromechanical analysis of woven fabric composites. AIAA 1983;21:1714–21.
[31] Middendorf P, Van Den Broucke B, Schouten M, Lomov SV, Verpoest I. Integrated simulation approach for textile composites. In: In Proceedings of SAMPE Technical, Madrid; 2007.
[32] Schouten M. Integrated tool for simulation of textile composites: ITOOL.. In: Proceedings of SEICO, Paris; 2007.
[33] Launay J, Hivet G, Duong AV, Boisse P. Experimental analysis of the influence of tensions on in plane shear behaviour of woven composite reinforcements. Compos Sci Technol 2008;68(2):506–15.
[34] Wille T, Hein R, Horn M, Knote A, Opitz M, Mayer N, Prowe J, Calomfirescu M, Balvers J, Apmann H. Development, implemenetation, and demonstration of a composite tool chain for concurrent engineering. In: Proceedings of NAFEMS world congress, Salzburg; 2013.
[35] Mayer N, Prowe J, Hinterhölzl R. Finite Element mapping for a structural analyisis of composites. In: Proceedings of ECCM16, Sevilla; 2014.
[36] Mayer N, Prowe J, Havar T, Hinterhölzl R, Drechsler K. Structural analysis of composite components considering manufacturing effect. Compos Struct 2016;140(15):776–82.
[37] Arya S, Mount D, Netanyahu N, Silverman R, Wu A. An optimal algorithm for approximate nearest neighbor searching in fixed dimensions. JACM 1998;45(6):891–923.
[38] Luo Y. A nearest-nodes finite element method with local multivariate lagrange interpolation. Finite Elem Anal Des 2008;44:797–803.
[39] Press WH, Teukolsky SA, Vetterling WT, Flannery BP. Numerical Recipes: The Art of Scientific Computing. 3 edition. Cambridge University Press; 2007. ISBN 978-0-521-88407-5.
[40] Prodromou AG, Chen J. On the relationship between shear angle and wrinkling of textile composite preforms. Compos Part A 1997;213A:491–503.
[41] Altmann A, Taubert R, Mandel U, Hinterhölzl R, Drechsler K. A continuum damage model to predict the influence of ply waviness on stiffness and strength in ultra-thick unidirectional Fiber-reinforced Plastics. J Compos Mater 2015;0(0):1–17.
[42] Long AC. Design and Manufacturing of Textile Composites. Woodhead Publishing Limited; 2005.
[43] Cox B, Flanagan G. Handbook of Analytical Methods for Textile Composites. Hampton (VA): National Aeronautics and Space Administration, Langley Research Center; 1997.
[44] Ivanov D, Lomov S. Compaction behaviour of dense sheared woven preforms: experimental observations and analytical predictions. Compos Part A 2014;64:167–76.
[45] Crookston J, Long A, Jones I. A summary review of mechanical properties prediction methods for textile reinforced polymer composites. Proc Inst Mech Eng, Part L – J Mater Des Appl 2005;219(L2):91–109.
[46] Crookston J. Prediction of elastic behaviour and initial failure of textile composites PhD thesis,. University of Nottingham; 2005.